Hindawi Publishing Corporation
Journal of Chemistry
Volume 2013, Article ID 959765, 6 pages
http://dx.doi.org/10.1155/2013/959765

Research Article

Ultrasound and Microwave Coassisted Synthesis and Luminescent Properties of $(Ca_{1-x}, Ln_x)MoO_4:Eu^{3+}$ (Ln = La, Gd; $0 < x < 0.5$) Phosphors

Jing Hu[1] and Qianming Wang[1,2,3]

[1] *School of Chemistry & Environment, South China Normal University, Guangzhou 510006, China*
[2] *Key Laboratory of Theoretical Chemistry of Environment, Ministry of Education, School of Chemistry & Environment, South China Normal University, Guangzhou 510006, China*
[3] *Guangdong Technology Research Center for Ecological Management and Remediation of Urban Water System, Guangzhou 510006, China*

Correspondence should be addressed to Qianming Wang; rareearth@126.com

Received 4 May 2013; Revised 26 July 2013; Accepted 15 August 2013

Academic Editor: Sylvain Franger

In order to control reaction temperature and reduce processing time, a new method of ultrasound irradiation with microwave heating was used to synthesize $(Ca_{1-x}, Ln_x)MoO_4:Eu^{3+}$ (Ln = La, Gd; $0 < x < 0.5$) phosphors at only 80°C in 30 minutes. Their crystal structures and morphologies which have been verified by X-ray diffraction (XRD) and scanning electron microscopy (SEM) exhibited gradual changes due to the insertion of lanthanide ions (La or Gd) in calcium molybdates. Codoping of lanthanum ions ($x = 0.2$) would enhance the emission intensities that were supported by fluorescent spectrophotometry (FL).

1. Introduction

Currently, rare earth molybdates have exhibited potential and widespread applications in the fields of luminescent materials with superior physical and chemical properties which have been attracting much attention [1–4]. Numerous methods of the synthesis processes have been developed and improved, such as the traditional solid-state method [5–7], sol-gel process [8, 9], or hydrothermal method [10–12]. However, most of the above treatments are complicated and have several technical problems, like relatively long reaction times, high temperatures, and massive energy supplies. Hence, the exploration of simple and convenient synthesis routes for energy saving and has been continued.

A promising method by combining the ultrasound and microwave irradiation together has been paid attention [13]. Ultrasonic forces during the precipitation reaction play a significant role on increasing chemical reactivity and improving chemical yields through the acoustic cavitations generated from the expansion of the insulation foams. The acoustic cavitations can produce the extremely high pressure and temperature in the reaction, thus providing a unique environment for the formation of chemical compounds with novel structures [14–17]. Microwave heating method is different from normal heating mode. It includes the following characteristics: heating uniformly and rapidly, low heat loss, and easy operation. Moreover, microwave heating technology not only can improve effectively the reaction conversion and selectivity, but also is one of the means to realize the green technology [18–20]. Therefore, we can combine the above two kinds of technology together to improve the synthetic scheme of the rare-earth molybdate compounds. Herein, in this paper, we synthesized a group of $(Ca_{1-x}, Ln_x)MoO_4:Eu^{3+}$ (Ln = La, Gd; $0 < x < 0.5$) phosphors via the supersonic

Scheme 1: Photo of the supersonic assisted microwave reactor.

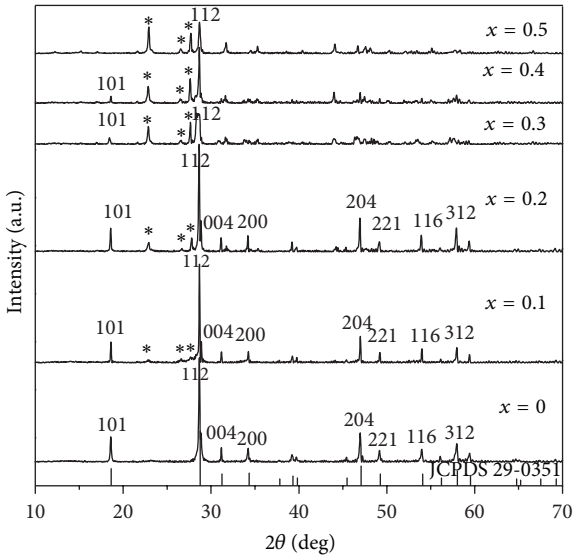

Figure 1: XRD patterns for $(Ca_{1-x}, La_x)MoO_4:Eu^{3+}$ (5 mol%) (x = 0, 0.1, 0.2, 0.3, 0.4, and 0.5) phosphors.

and microwave coassistance method without any surfactant or template. Their microstructures and photoluminescence properties were carefully studied.

2. Experimental Section

2.1. Materials and Methods. La_2O_3 (99.9%), Gd_2O_3 (99.9%), and Eu_2O_3 (99.9%) were purchased from Alfa Aesar company. $Ca(NO_3)_2{\cdot}4H_2O$ (99%), $(NH_4)_6Mo_7O_{24}{\cdot}4H_2O$ (99%), and ammonia water were provided by Aldrich company. Lanthanide nitrates were synthesized by dissolving the corresponding oxides in nitric acid solution. The supersonic assisted microwave reactor was manufactured by Nanjing Xianou Technology Company, China (XO-SM50). All the detailed experimental conditions were simply described here. Microwave power was set as 600 W, and reaction temperature was maintained at 80°C. Supersonic power remained to be 300 W with the reverse duty cycle of 2 s. All the operation time was set as 30 minutes. The picture of the machine in our lab was given in Scheme 1. The X-ray powder diffraction was measured on Bruker D8 diffractometer with Cu Kα radiation

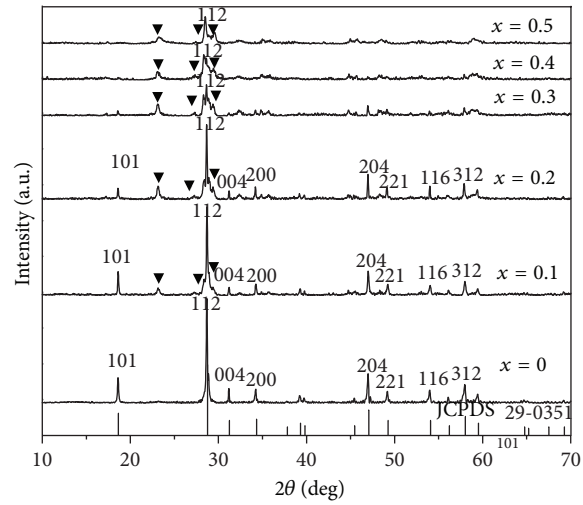

Figure 2: XRD patterns for $(Ca_{1-x}, Gd_x)MoO_4:0.05Eu^{3+}$ (x = 0, 0.1, 0.2, 0.3, 0.4, and 0.5) phosphors.

(λ = 0.1541 nm) in the range of 2θ = 20–80°. Scanning electronic microscope (SEM) was obtained with JSM-6360LV. Fluorescence spectra were obtained on an Edinburgh FLS920 spectrometer.

2.2. Synthesis of $(Ca_{1-x}, Ln_x)MoO_4:0.05Eu^{3+}$ (Ln = La, Gd). For the synthesis of $(Ca_{0.8}, La_{0.2})MoO_4:Eu^{3+}$ (5%) phosphors, $La(NO_3)_3$ (0.2 mmol), $Ca(NO_3)_3$ (0.8 mmol), and $Eu(NO_3)_3$ (0.05 mmol) were dissolved in water. Then the appropriate amount of ammonium heptamolybdate tetrahydrate, $(NH_4)_6Mo_7O_{24}{\cdot}4H_2O$, was dissolved in deionized water and added in the above solution. After the pH value of the above mixed solution was adjusted to about 7, the mixture was transferred to a three-neck flask which adapted to the reactor. Microwave power was set as 600 W, and reaction temperature was maintained at 80°C. Supersonic power remained to be 300 W with the reverse duty cycle of 2 s. All the operation time was set as 30 minutes. Finally, the precipitates were retrieved by centrifugation, washed by deionized water several times, and then dried at 60°C in vacuum for 24 h. Meanwhile, a series of $(Ca_{1-x}, Ln_x)MoO_4:0.05Eu^{3+}$ (Ln = La, Gd; $0 < x < 0.5$) phosphors was prepared by a similar procedure.

3. Results and Discussion

3.1. Structural Analysis. Because the crystal structure, morphologies, and sizes of samples have an enormous impact on the photophysical properties, the crystal structure, morphologies, and sizes of $(Ca_{1-x}, Ln_x)MoO_4:Eu^{3+}$ (5 mol%) (Ln = La, Gd; $0 < x < 0.5$) (x = 0, 0.1, 0.2, 0.3, 0.4, and 0.5) phosphors obtained by ultrasonic and microwave assisted method were investigated by X-ray diffraction (XRD) and scanning electronic microscope (SEM), respectively. Figure 1 is the crystalline phases of $(Ca_{1-x}, La_x)MoO_4:Eu^{3+}$ (5 mol%) (x = 0, 0.1, 0.2, 0.3, 0.4, and 0.5) samples. It can be seen that the Bragg reflection peaks of $CaMoO_4:Eu^{3+}$ (5 mol%)

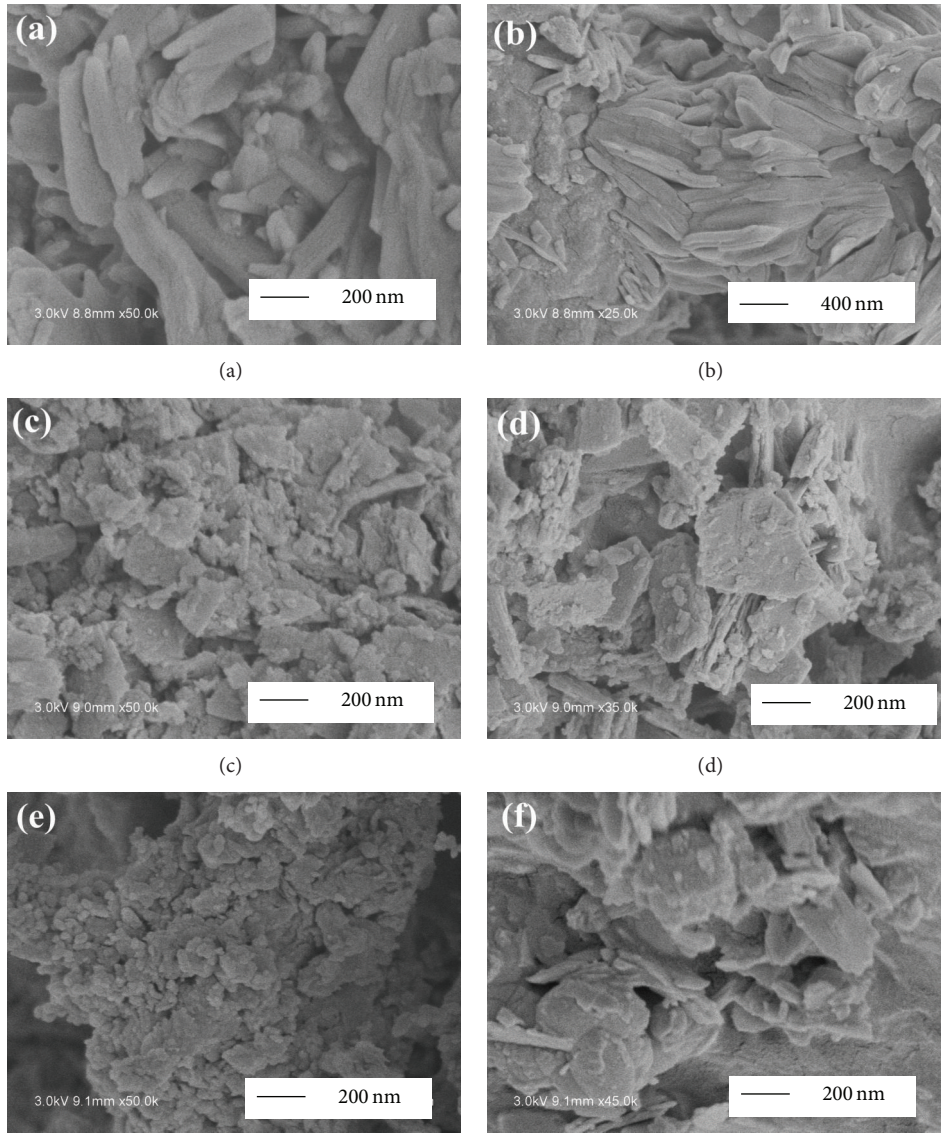

FIGURE 3: SEM images of $(Ca_{1-x}, Ln_x)MoO_4{:}0.05Eu^{3+}$ (Ln = La and Gd) phosphors: (a) and (b) $CaMoO_4{:}0.05Eu^{3+}$, (c) $(Ca_{0.8}, La_{0.2})MoO_4{:}0.05Eu^{3+}$, (d) $(Ca_{0.5}, La_{05})MoO_4{:}0.05Eu^{3+}$, (e) $(Ca_{0.8}, Gd_{0.2})MoO_4{:}0.05Eu^{3+}$, and (f) $(Ca_{0.5}, Gd_{0.5})MoO_4{:}0.05Eu^{3+}$.

correspond to the structure similar to the Joint Committee on Powder Diffraction Standards (JCPDS) file 29-0351 of $CaMoO_4$ with a tetragonal phase and space group $I41/a$ ($a = b = 5.226$ Å, $c = 11.430$ Å), which demonstrates that the doped europium ion cannot change the crystal structure. The patterns of XRD indicate that the structure of $(Ca_{1-x}, La_x)MoO_4{:}Eu^{3+}$ (5 mol%) matches well with calcium molybdates when x was less than 0.2. The further increasing amounts of lanthanum still maintain the primary crystal structure, and the new peak at 23° grows very fast, suggesting that replacement of calcium ions by agglomeration of lanthanum ions may trigger the lattice distortion and partial phase changes. This stepwise difference also induced microstructure transformation and luminescence changes as indicated by the following measurements. It is worthy to mention that such a short reaction time (30 min) will be very efficient and superior to other synthetic processes such as hydrothermal method that needs more than 10 hours. A similar investigation was performed for $(Ca_{1-x}, Gd_x)MoO_4{:}0.05Eu^{3+}$ with $x = 0$, 0.1, 0.2, 0.3, 0.4, and 0.5. Figure 2 is the XRD patterns of those phosphors. As the gadolinium contents continually increase up to 0.5, the structures of samples have some changes and the relative intensity of diffraction peaks becomes weaker. Compared with $(Ca_{1-x}, La_x)MoO_4{:}Eu^{3+}$ (5 mol%), the changes triggered by the insertion of gadolinium were more obvious because the ionic radius of Gd^{3+} (93.8 pm) was much smaller than lanthanum (106.1 pm) when they replaced large calcium ions (114 pm).

In order to investigate the influence of La^{3+} and Gd^{3+} content on the morphologies and sizes of samples prepared by ultrasound and microwave coassisted method, the SEM

images are given in Figure 3. Figures 3(a)–3(f) are the SEM images of $(Ca_{1-x}, Ln_x)MoO_4:Eu^{3+}$ (5 mol%) (Ln = La, Gd) phosphors with $x = 0$, 0.2, and 0.5, respectively. Figures 3(a) and 3(b) revealed that the shape formed shows a relatively orderly alignment of rod-like structures with the length at about 1 μm. A sheet-like structure was observed next in Figure 3(c) when lanthanum ions were doped into the materials. The shape evolution due to the continuous addition of lanthanum elements was provided in Figure 3(d), and the size for the sheets grew into large aggregates. The reproducibility of the formation of this structure was also confirmed in the analogous samples of $(Ca_{1-x}, Gd_x)MoO_4:Eu^{3+}$ (5 mol%) (Figures 3(e) and 3(f)).

3.2. Photophysical Properties. For the sake of studying the effect of concentration of La^{3+} and Gd^{3+} on the photophysical properties, we have carefully carried out a series of experiments with the formula of $(Ca_{1-x}, Ln_x)MoO_4:Eu^{3+}$ (5 mol%) (Ln = La, Gd) (x = 0.1, 0.2, 0.3, 0.4, and 0.5) prepared by ultrasonic and microwave coassisted method at a low temperature of 80°C in 30 minutes.

The excitation spectrum of $(Ca_{1-x}, La_x)MoO_4:Eu^{3+}$ (5 mol%) (x = 0.2) phosphors was obtained by monitoring the emission wavelength at 616 nm under room temperature (Figure 4). Other samples show similar excitation feature except for difference intensity. A broad luminescence band ranging from 220 to 350 nm with the maximum at about 276 nm in the spectrum is attributed to charge transfer from oxygen to molybdenum atom. Other narrow and sharp peaks centered at 364, 383, 395, 417, 465 nm were assigned to intraconfigurational f-f transitions ($^7F_0 \rightarrow {}^5D_4$, $^7F_0 \rightarrow {}^5G_2$, $^7F_0 \rightarrow {}^5L_6$, $^7F_0 \rightarrow {}^5D_3$, and $^7F_0 \rightarrow {}^5D_2$, resp.) of Eu^{3+} in the host of molybdate.

The emission spectra of red phosphors $(Ca_{1-x}, La_x)MoO_4:Eu^{3+}$ (5 mol%) with various concentration of La^{3+} (the monitoring wavelength is about 276 nm) are shown in Figure 4. All sharp emission lines in the emission spectra correspond to the electronic transitions as $^5D_0 \rightarrow {}^7F_1$ (593 nm), $^5D_0 \rightarrow {}^7F_2$ (615 nm), $^5D_0 \rightarrow {}^7F_3$ (656 nm), and $^5D_0 \rightarrow {}^7F_4$ (707 nm), respectively, and the most intense and sensitive emission lines at about 616 nm for electric-dipole transition ($^5D_0 \rightarrow {}^7F_2$) indicate that europium ion does not occupy the center of symmetry [21, 22]. The influence of mole percent of La^{3+} on the intensity of phosphors can be found from Figures 4 and 5. Along with the increasing amounts of La^{3+}, the luminescent intensity reaches maximum at 0.2, then becomes weakened from 0.3 to 0.5. It is known that the ionic radii of trivalent lanthanide ions are similar to Ca^{2+}; therefore, the lower doping contents of La^{3+} replacing lattice position of calcium will contribute to the europium(III) emissions. However, the association constants of lanthanide complexes are significantly higher than calcium complex. The lanthanide ions have a larger hydration sphere than Ca^{2+}, and the ability of La^{3+} to accommodate ligands will be stronger than calcium. Accordingly, the concentrated lanthanum ions will easily cause particle agglomeration which could be seen in SEM images, and the europium luminescence might be quenched by aggregation effects.

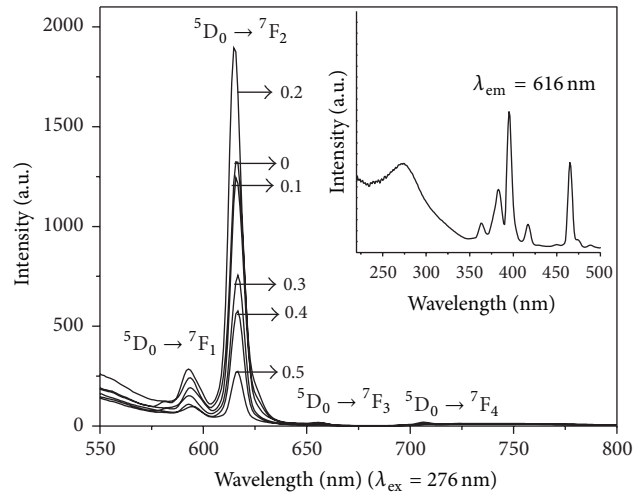

FIGURE 4: Emission spectra of $(Ca_{1-x}, La_x)MoO_4:0.05Eu^{3+}$ (x = 0.1, 0.2, 0.3, 0.4, and 0.5) phosphors (λ_{ex} = 276 nm) with excitation spectrum of $(Ca_{0.8}, La_{0.2})MoO_4:0.05Eu^{3+}$ phosphor λ_{em} = 616 nm (inset).

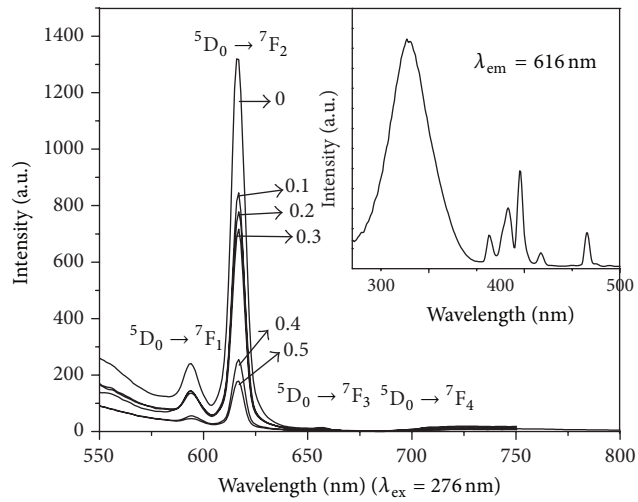

FIGURE 5: Emission spectra of $(Ca_{1-x}, Gd_x)MoO_4:0.05Eu^{3+}$ (x = 0.1, 0.2, 0.3, 0.4, and 0.5) phosphors (λ_{ex} = 276 nm) with excitation spectrum of $(Ca_{0.1}, Gd_{0.9})MoO_4:Eu^{3+}$ (5 mol%) phosphors (λ_{em} = 615 nm, inset).

As shown in Figure 5, the excitation spectrum of $(Ca_{1-x}, Gd_x)MoO_4:0.05Eu^{3+}$ (x = 0.1) phosphors was measured at about 616 nm, and the emission spectra of $(Ca_{1-x}, Gd_x)MoO_4:Eu^{3+}$ (5 mol%) (x = 0.1, 0.2, 0.3, 0.4, and 0.5) phosphors were obtained at about 276 nm. As shown in Figure 5, the excitation spectrum consists of a broad and strong band of O^{2-}-Mo^{6+} charge transfer transition ranging from 220 nm to 350 nm and several narrow peaks for internal energy levels transition of Eu^{3+} within wavelength range of 350 nm to 500 nm. Upon excitation at 276 nm, it can be seen that the strong emission is at about 616 nm due to $^5D_0 \rightarrow {}^7F_2$ indicating that europium ion is located in a low symmetric

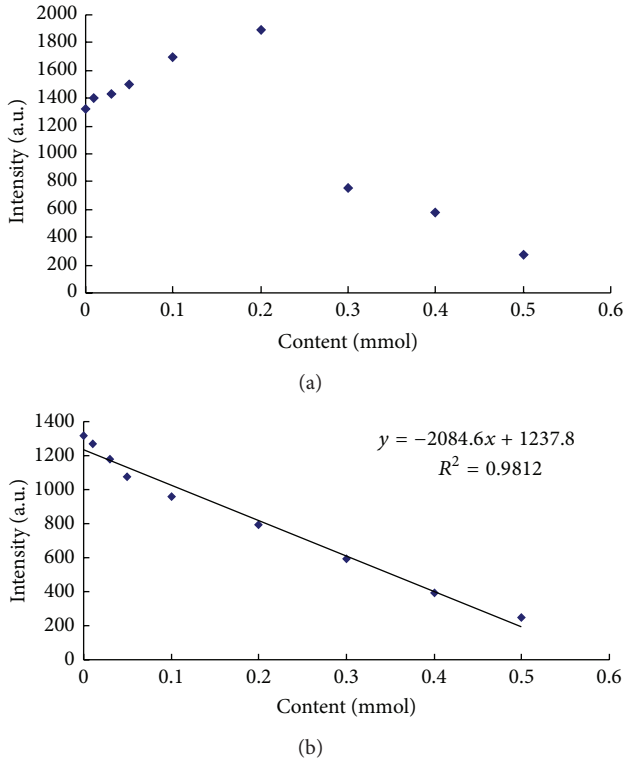

FIGURE 6: Effect of the different contents of La^{3+} (a) and Gd^{3+} (b) on the luminescent properties of the red-emitting phosphors.

site, and other relatively weak peaks in the wavelength range of 550–750 nm correspond to other transitions from $^5D_0$ to ^7F_J ($J = 1, 2, 3, 4$). From Figure 6, it can be obviously seen that the correlation between the intensity and the contents of Gd^{3+} followed a linear equation $Y = -2084.6X + 1237.8$ ($R^2 = 0.9812$).

4. Conclusions

In brief, $(Ca_{1-x}, Ln_x)MoO_4:Eu^{3+}$ (5 mol%) (Ln = La, Gd; $0 < x < 0.5$) phosphors have been successfully synthesized by an ultrasound and microwave coassisted method at low temperature of 80°C in 30 min. The XRD and SEM results show that the La, Gd doped phosphors can gradually change the crystalline structures, and the sizes of those powders grew larger. The as-prepared materials were red emissive, and the doped concentrations of La^{3+} are optimized as 0.2 and 0.1, respectively. The above mentioned materials may be useful as luminescent probes in biomedical science and in light-emitting diodes applications.

Conflict of Interests

All the authors confirm that there is no conflict of interests with any financial organization regarding the materials or equipments mentioned in the paper.

Acknowledgments

Q. M. appreciates the National Natural Science Foundation of China (21002035).

References

[1] L. Li, W. Zi, G. Li et al., "Hydrothermal synthesis and luminescent properties of $NaLa(MoO_4)_2:Dy^{3+}$ phosphor," *Journal of Solid State Chemistry*, vol. 191, pp. 175–180, 2012.

[2] A. Kumar and J. Kumar, "Perspective on europium activated fine-grained metal molybdate phosphors for solid state illumination," *Journal of Materials Chemistry*, vol. 21, no. 11, pp. 3788–3795, 2011.

[3] J. Zhang, X. Wang, X. Zhang, X. Zhao, X. Liu, and L. Peng, "Microwave synthesis of $NaLa(MoO_4)_2$ microcrystals and their near-infrared luminescent properties with lanthanide ion doping (Er^{3+}, Nd^{3+}, Yb^{3+})," *Inorganic Chemistry Communications*, vol. 14, no. 11, pp. 1723–1727, 2011.

[4] A. Tang, D.-F. Zhang, and L. Yang, "Photoluminescence characterization of a novel red-emitting phosphor $In_2(MoO_4)_3:Eu^{3+}$ for white light emitting diodes," *Journal of Luminescence*, vol. 132, no. 6, pp. 1489–1492, 2012.

[5] W. Zhao, W. Zhou, M. Song et al., "Spectroscopic investigation of Dy^{3+}-doped $Li_2Gd_4(MoO_4)_7$ crystal for potential application in solid-state yellow laser," *Journal of Alloys and Compounds*, vol. 509, no. 9, pp. 3937–3942, 2011.

[6] J. Wan, L. Cheng, J. Sun et al., "Energy transfer and colorimetric properties of Eu^{3+}/Dy^{3+} co-doped $Gd_2(MoO_4)_3$ phosphors," *Journal of Alloys and Compounds*, vol. 496, no. 1-2, pp. 331–334, 2010.

[7] Z. Lin, X. Han, and C. Zaldo, "Solid state reaction synthesis and optical spectroscopy of ferroelectric $(Gd_{1-x}Ln_x)_2(MoO_4)_3$; with Ln = Yb or Tm," *Journal of Alloys and Compounds*, vol. 492, no. 1-2, pp. 77–82, 2010.

[8] C. Guo, T. Chen, L. Luan, W. Zhang, and D. Huang, "Luminescent properties of $R_2(MoO_4)_3:Eu^{3+}$ (R = La, Y, Gd) phosphors prepared by sol-gel process," *Journal of Physics and Chemistry of Solids*, vol. 69, no. 8, pp. 1905–1911, 2008.

[9] J. Liao, D. Zhou, B. Yang, R. Liu, Q. Zhang, and Q. Zhou, "Sol-gel preparation and photoluminescence properties $CaLa_2(MoO_4)_4:Eu^{3+}$ phosphors," *Journal of Luminescence*, vol. 134, pp. 533–538, 2013.

[10] J. C. Sczancoski, L. S. Cavalcante, M. R. Joya, J. A. Varela, P. S. Pizani, and E. Longo, "$SrMoO_4$ powders processed in microwave-hydrothermal: synthesis, characterization and optical properties," *Chemical Engineering Journal*, vol. 140, no. 1–3, pp. 632–637, 2008.

[11] L. S. Cavalcante, J. C. Sczancoski, M. Siu Li, E. Longo, and J. A. Varela, "β-$ZnMoO_4$ microcrystals synthesized by the surfactant-assisted hydrothermal method: growth process and photoluminescence properties," *Colloids and Surfaces A*, vol. 396, pp. 346–351, 2012.

[12] Q.-M. Wang and B. Yan, "Hydrothermal mild synthesis of microrod crystalline $Y_xGd_{2-x}(MoO_4)_3:Eu^{3+}$ phosphors derived from facile co-precipitation precursors," *Materials Chemistry and Physics*, vol. 94, no. 2-3, pp. 241–244, 2005.

[13] D. Li, J. Wang, X. Wu, C. Feng, and X. Li, "Ultraviolet-assisted synthesis of hourglass-like ZnO microstructure through an ultrasonic and microwave combined technology," *Ultrasonics Sonochemistry*, vol. 20, no. 1, pp. 133–136, 2013.

[14] M. A. Patel, B. A. Bhanvase, and S. H. Sonawane, "Production of cerium zinc molybdate nano pigment by innovative ultrasound assisted approach," *Ultrasonics Sonochemistry*, vol. 20, no. 3, pp. 906–913, 2013.

[15] A. Gedanken, "Doping nanoparticles into polymers and ceramics using ultrasound radiation," *Ultrasonics Sonochemistry*, vol. 14, no. 4, pp. 418–430, 2007.

[16] L. Zhu, Y. Liu, X. Fan, D. Yang, and X. Cao, "Rapid synthesis of single-crystalline TbF_3 with novel nanostructure via ultrasound irradiation," *Materials Research Bulletin*, vol. 46, no. 2, pp. 252–257, 2011.

[17] Y. Wang, L. Yin, and A. Gedanken, "Sonochemical synthesis of mesoporous transition metal and rare earth oxides," *Ultrasonics Sonochemistry*, vol. 9, no. 6, pp. 285–290, 2002.

[18] C. Badan, O. Esenturk, and A. Yilmaz, "Microwave-assisted synthesis of Eu^{3+} doped lanthanum orthoborates, their characterizations and luminescent properties," *Solid State Sciences*, vol. 14, no. 11-12, pp. 1710–1716, 2012.

[19] K. Uematsu, K. Toda, and M. Sato, "Preparation of YVO_4:Eu^{3+} phosphor using microwave heating method," *Journal of Alloys and Compounds*, vol. 389, no. 1-2, pp. 209–214, 2005.

[20] T. T. Huong, V. D. Tu, T. K. Anh, L. T. Vinh, and L. Q. Minh, "Fabrication and characterization of YVO_4:Eu^{3+} nanomaterials by the micro-wave technique," *Journal of Rare Earths*, vol. 29, no. 12, pp. 1137–1141, 2011.

[21] X. Zhang, C. Zhang, H. Guo et al., "Optical spectra of a novel polyoxometalate occluded within modified MCM-41," *Journal of Physical Chemistry B*, vol. 109, no. 41, pp. 19156–19160, 2005.

[22] N. Zhang, W. Bu, Y. Xu, D. Jiang, and J. Shi, "Self-assembled flowerlike europium-doped lanthanide molybdate microarchitectures and their photoluminescence properties," *Journal of Physical Chemistry C*, vol. 111, no. 13, pp. 5014–5019, 2007.